2014

# Accelerated Flooding Along the U.S. East Coast: On the Impact of Sea-Level Rise, Tides, Storms, the Gulf Stream, and the North Atlantic Oscillations

Tal Ezer
*Old Dominion University*, tezer@odu.edu

Larry P. Atkinson
*Old Dominion University*, latkinso@odu.edu



## Original Publication Citation

Ezer, T., & Atkinson, L.P. (2014). Accelerated flooding along the U.S. East Coast: On the impact of sea-level rise, tides, storms, the Gulf Stream, and the North Atlantic Oscillations. *Earth's Future, 2*(8), 362-382. doi: 10.1002/2014EF000252

AGU PUBLICATIONS

Earth's Future

RESEARCH ARTICLE
10.1002/2014EF000252

**Key Points:**
- Flooding is accelerating on U.S. East Coast
- Sea-level rise and tidal range impact flooding
- North Atlantic Oscillations and Gulf Stream impact flooding

**Corresponding author:**
T. Ezer, tezer@odu.edu

**Citation:**
Ezer, T., and L. P. Atkinson (2014), Accelerated flooding along the U.S. East Coast: On the impact of sea-level rise, tides, storms, the Gulf Stream, and the North Atlantic Oscillations, *Earth's Future*, *2*, 362–382, doi:10.1002/2014EF000252.

Received 2 MAY 2014
Accepted 11 JUL 2014
Accepted article online 16 JUL 2014
Published online 11 AUG 2014



# Accelerated flooding along the U.S. East Coast: On the impact of sea-level rise, tides, storms, the Gulf Stream, and the North Atlantic Oscillations

**Tal Ezer[1] and Larry P. Atkinson[1]**

[1]Center for Coastal Physical Oceanography, Old Dominion University, Norfolk, Virginia, USA

**Abstract** Recent studies identified the U.S. East Coast north of Cape Hatteras as a "hotspot" for accelerated sea-level rise (SLR), and the analysis presented here shows that the area is also a "hotspot for accelerated flooding." The duration of minor tidal flooding [defined as 0.3 m above MHHW (mean higher high water)] has accelerated in recent years for most coastal locations from the Gulf of Maine to Florida. The average increase in annual minor flooding duration was ~20 h from the period before 1970 to 1971–1990, and ~50 h from 1971–1990 to 1991–2013; spatial variations in acceleration of flooding resemble the spatial variations of acceleration in sea level. The increase in minor flooding can be predicted from SLR and tidal range, but the frequency of extreme storm surge flooding events (0.9 m above MHHW) is less predictable, and affected by the North Atlantic Oscillations (NAO). The number of extreme storm surge events since 1960 oscillates with a period of ~15 year and interannual variations in the number of storms are anticorrelated with the NAO index. With higher seas, there are also more flooding events that are unrelated to storm surges. For example, it is demonstrated that week-long flooding events in Norfolk, VA, are often related to periods of decrease in the Florida Current transport. The results indicate that previously reported connections between decadal variations in the Gulf Stream (GS) and coastal sea level may also apply to short-term variations, so flood predictions may be improved if the GS influence is considered.

## 1. Introduction

High relative sea-level rise (SLR) rates recorded by tide gauges along the U.S. East Coast (Figure 1) and sea-level acceleration north of Cape Hatteras, NC [*Boon*, 2012; *Ezer and Corlett*, 2012; *Sallenger et al*., 2012; *Ezer*, 2013; *Ezer et al*., 2013; *Kopp*, 2013] are expected to increase coastal flooding associated with tides and storm surges. The Mid-Atlantic coastal region has been called a "hot spot of accelerated SLR," and positive acceleration has been calculated by at least four different statistical methods [*Boon*, 2012; *Ezer and Corlett*, 2012; *Sallenger et al*., 2012; *Kopp*, 2013]. However, how to detect statistically significant sea-level acceleration is still being debated [*Haigh et al*., 2014], and uncertainties remain about the implications of sea-level acceleration for the likelihood of future flooding and coastal risk management issues [*Nicholls and Cazenave*, 2010; *Cazenave and Cozannet*, 2014]. Therefore, we will show here that acceleration in flooding extent is more clearly detectable than acceleration in SLR rates; both accelerations are correlated with each other and show similar spatial patterns along the coast. Moreover, flooding statistics, as presented in this study, are useful for practical purposes of developing flood mitigation strategies. Several low-lying populated regions along the U.S. coasts are especially vulnerable to SLR, including south Florida [*Zhang*, 2011] and the Hampton Roads region in the lower Chesapeake Bay [*Kleinosky et al.,* 2007; *Atkinson et al*., 2013; *Boesch et al*., 2013; *Mitchell et al*., 2013]. In addition to large land subsidence around the Chesapeake Bay area due to glacial isostatic adjustment (GIA) [*Boon et al*., 2010; *Kopp*, 2013], SLR acceleration in the Mid-Atlantic coastal region has been found to be highly correlated with recent offshore shift and weakening in the Gulf Stream (GS) just north of Cape Hatteras, as seen in altimeter data [*Ezer et al*., 2013] and in direct observations of the Florida Current (FC) [*Ezer*, 2013]. The latter finding is consistent with dynamic sea-level changes seen in ocean models [*Ezer*, 1999, 2001; *Levermann et al*., 2005; *Yin et al*., 2009; *Yin and Goddard*, 2013] and expected weakening in the Atlantic Meridional Overturning Circulation (AMOC) under warmer climate conditions [*Hakkinen and Rhines*, 2004; *McCarthy et al*., 2012; *Sallenger et al*., 2012; *Srokosz et al*., 2012; *Smeed et al*., 2013]. Although the long-term weakening of the GS is still small and


**Figure 1.** Map of the U.S. East Coast (based on Google Earth) and location of tide gauge stations.

difficult to detect [*Rossby et al*., 2014], variations on scales ranging from weeks to decades may result in large temporal and spatial variations of SLR rates along the U.S. East Coast [*Ezer*, 2013; *Kopp*, 2013].

The motivation for our study comes from the fact that temporal and spatial variations in sea level pose challenging questions on how to assess the flooding risk of coastal regions. For example, it is well recognized that a storm surge larger than normal may occur if a hurricane landfall coincides with high tide (e.g., when storm Sandy hit New Jersey and New York in 2012), but less understood is the possibility that a storm surge coincides with a period of relatively higher sea level due to seasonal variations or a weaker GS [*Sweet et al*., 2009]. Periods of anomalous high water can last weeks or months [*Sweet et al*., 2009], and possibly years or decades [*Ezer*, 2013; *Ezer et al*., 2013]. There are numerous studies that assess the risk of extreme events, for example, *Kemp and Horton* [2013] studied the contribution of SLR and high tide timing to hurricane flooding in New York City over the past ~200 years, while *Zhang and Sheng* [2013] used observations and numerical model simulations to study the contribution of storms and tides to extreme sea-level events along the eastern coast of North America. The latter study did not consider the impact of SLR, and neither study considered the impact of changes in ocean dynamics or the GS. For each tide gauge in the United States, NOAA provides statistics of 1%, 10%, 50%, and 99% annual exceedance probability (tidesandcurrents.noaa.gov). For example, 1% exceedance probability means that the likelihood of water level reaching particular water level in any year is in average 1/100; an extreme storm surge event of this type is "the average recurrence interval" [see *Hunter*, 2010 for definitions]. But how to interpret such information or use it for risk management or mitigation planning is not always clear. Moreover, the NOAA exceedance statistics is based on the average of past measurements, so it does not consider how the likelihood of flooding has changed in the past and how it will change in the future due to the impact of SLR. A simple statistical method to estimate the expected exceedance under future SLR has been offered by *Hunter* [2012]. However, in this study, we do not attempt to calculate probability statistics of sea level, as it has already been done by other studies mentioned above. Instead, we provide more practical information on the duration of (potential) flooding when water level reached a particular level and how the likelihood of floods change over time and space. Moreover, while most other studies focus on extreme storm surge events, we also provide flood statistics for minor and moderate tidal flooding events that are not catastrophic, but very important for people living near waterfronts and coasts. Such information was found to be very useful to communicate flood risks to the local population and planners in the flood-prone region around the city of Norfolk, VA [*Atkinson et al*., 2013] and along the shores of the Chesapeake Bay [*Boesch et al*., 2013; *Mitchell et al*., 2013].

Observed coastal relative sea level at a particular time ($t$) and location ($x$) is the result of several components,

$$h(x,t) = \mathrm{DAT}(x) + \mathrm{GLB}(t) + \mathrm{SUB}(x,t) + \mathrm{LOC}(x,t) + \mathrm{TID}(x,t) + \mathrm{STO}(x,t)\,. \quad (1)$$

Each component has different temporal (T) and spatial (X) scales: DAT is a reference datum (the current National Tidal Datum Epoch is based on averages for 1983–2001), GLB is the global SLR (T ~ decades to centuries), SUB is the local land subsidence due to GIA (X ~ 100–1000 km; T ~ 1000s of years), LOC is local

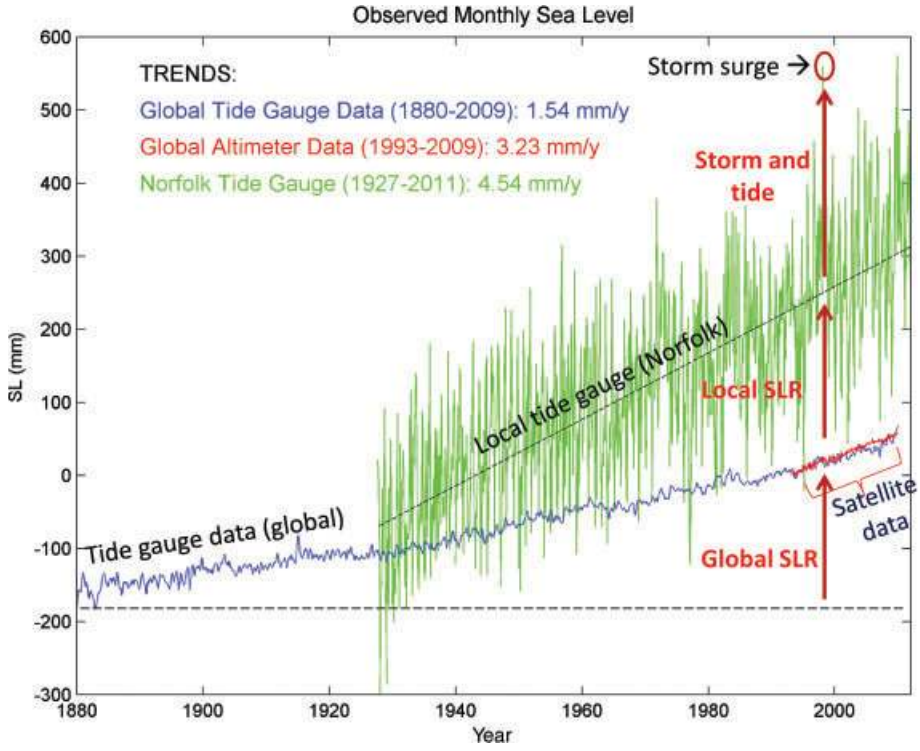


**Figure 2.** Comparison of monthly sea level in Norfolk (green) with global mean sea level obtained from tide gauges (blue) and AVISO satellite altimeters (red). The different contributions to a storm surge event are illustrated. See *Ezer* [2013] for information on the global data sets.

changes due to groundwater extraction, weather pattern, ocean dynamics, changes in gravity field due to mass redistribution, and other processes not homogeneous in space (X ~ 10s–100s km; T ~ days to years), TID is the tidal contribution (T ~ hours to days), and STO is major storm surge events (T ~ months to years). For short-term sea-level variations, GLB, SUB, and TID contributions are the most predictable and the LOC and STO the most unpredictable.

Figure 2 shows an example of the different contributions to a high-water storm event in Norfolk, where the local SLR is ~1.5 times larger than the altimeter-derived global mean sea level of the past ~20 years and ~3 times larger than the tide-gauge-derived [*Church and White*, 2011] global mean SLR of the past century. In the past, GIA was responsible for the large local SLR in Norfolk [*Boon et al*., 2010], but additional acceleration in SLR in recent years may be due to weakening of the GS since ~2004 according to *Ezer et al*. [2013], so one needs to assess the impact of these changes in ocean currents on potential flooding. We define a storm surge event as a period when water level reached a particular level above mean higher high water (MHHW). For example, Figure 3 shows that 17 extreme storm surge events occurred in Norfolk over the past 85 years, when water level reached at least 0.9 m (~3 feet) above MHHW. The impact of SLR is also demonstrated in Figure 3—the top storm surge was caused by the Chesapeake-Potomac Hurricane of 1933 when sea level was ~0.4 m lower than today, so a storm surge with similar strength if occurring today could cause water level to reach ~2 m above MHHW. Note also that, more than half of the big storm surges occurred during the past 15 years, but only one storm occurred in a 35 year span, between 1963 and 1997 suggesting that SLR as well as decadal variations may affect the frequency of storm events. The changing frequency of storm events will thus be addressed in this study. However, the frequency of storm events and the maximum water level reached for each storm do not accurately represent the flooding risk and damage. For example, the most flooding in Norfolk happened during the "Veterans Day Northeaster" of 2009 because floods lasted for several tidal cycles when water continued to flow into more streets compared with much stronger hurricanes when water receded immediately after the storm passed. To capture this phenomenon, from hourly sea-level data, $h(t)$, the total hours of flooding

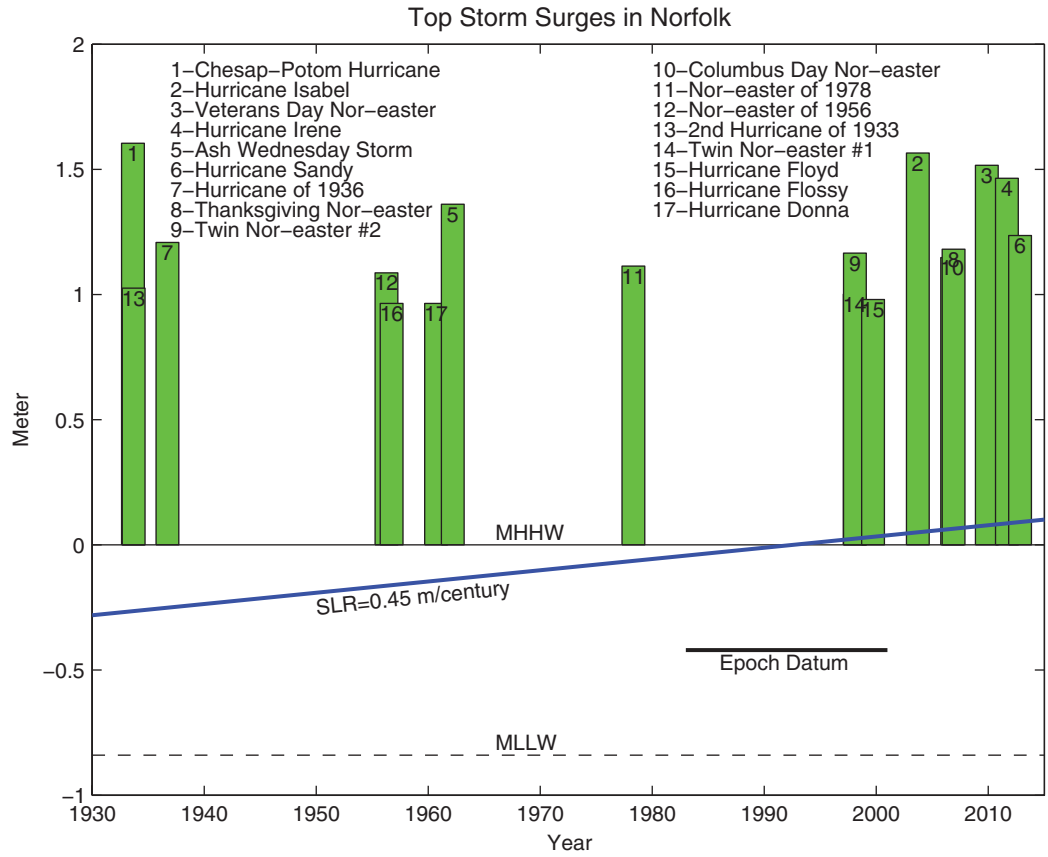


**Figure 3.** Maximum measured water level (relative to MHHW, defined by the mean of the epoch period 1982–2001) at Sewells Point, Norfolk, VA, during the top 17 storm surges. The sea-level rise during the observed period is indicated by the blue line. The total amplitude of the storm surge relative to the mean water level at the time of the storm is the difference between the top of the green bar and the blue line.

per year ($T$) for each station ($i$) are calculated for three selected critical water levels (WLc above MHHW),

$$T_i^{\text{year}} = \sum_{\text{year}} t \;\; ; \;\; h(t) > \text{WLc}, \;\; \text{WLc} = 0.3,\;\; 0.6,\;\; 0.9\,\text{m}. \tag{2}$$

Local topography and coastal slopes may result in a nonlinear relation between SLR and actual inundation [*Zhang*, 2011], so a more detailed analysis is needed to determine if a particular place will be flooded or not. However, the three categories of flooding defined by WLc roughly represent (e.g., in downtown Norfolk) minor tidal flooding (i.e., sometimes referred to as "nuisance flooding" with wet streets), moderate weather-related flooding (e.g., a weather front passing during Spring tide), and extreme storm events (e.g., a hurricane or major nor'easter), respectively. The calculations based on equation (2) are directly related to the exceedance probability and the average recurrence interval [e.g., see *Hunter*, 2010 for definitions]; the higher the WLc, the lower the recurrence interval is. However, as exceedance probability is routinely calculated by NOAA, it is not repeated here. Instead, analyzing how flooding frequency and duration change between different locations and how they are affected by the different components in equation (1), as well as by large-scale Atlantic Ocean variations, are the main goals of this study.

## 2. Sea-Level Data

Hourly sea-level records from 11 tide gauge stations were obtained from NOAA (http://opendap.co-ops.nos.noaa.gov/dods/). The locations are shown in Figure 1 and information on each station, including tidal range and SLR, is listed in Table 1. The data cover four different regions along the U.S. coast, three stations in the Gulf of Maine, four stations in the Mid-Atlantic Bight, three stations in the South Atlantic

**Table 1.** Information About the Hourly Sea-Level Data Used in This Study and the Calculated Statistics[a]

| Station Name, Location, and Starting Hourly Data (All End in 2013) | | | | Sea-Level Statistics | | | | | |
|---|---|---|---|---|---|---|---|---|---|
| | | | | Tidal range (m) | SLR (mm yr$^{-1}$) | h yr$^{-1}$ of WL > 0.3 m | | | |
| | Lat (°N) | Lon (°W) | *Y*1 | MHHW − MLLW | Mean ± 95% CI | *Y*1-1970 | 1971–1990 | 1991–2013 | ACC (h yr$^{-2}$) |
| 1. Eastport, ME | 44.90 | 66.98 | 1958 | 5.87 | 1.93 ± 0.55 | 127 | 110 | 183 | 0.24 |
| 2. Portland, ME | 43.66 | 70.25 | 1911 | 3.02 | 1.89 ± 0.20 | 38 | 79 | 109 | 0.013 |
| 3. Boston, MA | 42.35 | 71.05 | 1922 | 3.13 | 2.79 ± 0.24 | 40 | 71 | 116 | 0.045 |
| 4. Battery, NY | 40.70 | 74.01 | 1920 | 1.54 | 3.12 ± 0.23 | 19 | 41 | 99 | 0.076 |
| 5. Atlantic City, NJ | 39.36 | 74.42 | 1912 | 1.40 | 4.16 ± 0.20 | 12 | 33 | 94 | 0.078 |
| 6. Lewes, DE | 38.78 | 75.12 | 1967 | 1.42 | 3.82 ± 0.73 | 31 | 33 | 89 | 0.150 |
| 7. Norfolk, VA | 36.95 | 76.33 | 1927 | 0.84 | 4.54 ± 0.26 | 19 | 39 | 128 | 0.136 |
| 8. Wilmington, NC | 34.23 | 77.95 | 1938 | 1.43 | 2.01 ± 0.33 | 2.5 | 6 | 28 | 0.038 |
| 9. Charleston, SC | 32.78 | 79.93 | 1922 | 1.76 | 3.15 ± 0.24 | 12 | 27 | 71 | 0.060 |
| 10. Ft. Pulaski, GA | 32.03 | 80.90 | 1921 | 2.29 | 3.16 ± 0.23 | 19 | 41 | 99 | 0.076 |
| 11. Key West, FL | 24.56 | 81.81 | 1913 | 0.55 | 2.39 ± 0.20 | 4 | 4.5 | 13 | 0.013 |
| Mean ± SD | | | 87 years | 1.92 ± 0.8 | 3.00 ± 0.9 | 21 ± 13 | 41 ± 22 | 92 ± 29 | |

[a]The mean high tidal range is defined as the difference between MHHW and MLLW. The mean sea-level rise (SLR) obtained from linear regression and the 95% confidence interval is estimated based on *Zervas* [2009]. The minor flooding estimate for different periods is based on the hours per year with water level at least 0.3 m over MHHW; the two stations in the extreme north and south were neglected in the calculations of the mean flooding of all stations (last four columns of the bottom row). ACC is the estimated acceleration in flooding time [see equation (3) in text].

Bight, and one station (Key West) between the Florida Strait and the Gulf of Mexico (Figure 1). Only stations with relatively long and continuous hourly records were used, with an average period of 87 years. These stations represent large variations in tidal range, from ~0.5 m (the southernmost point, Key West, FL) to ~6 m (the northernmost point, Eastport, ME). With these data, the impact of tidal range on flooding can be evaluated. The mean (relative) SLR rate varies from ~1.9 mm yr$^{-1}$ (Gulf of Maine) to ~4–5 mm yr$^{-1}$ (lower Mid-Atlantic Bight). Most studies of SLR use monthly data, which may cover in some stations longer records than the hourly data, so the SLR rates in Table 1 are slightly different than those reported by *Ezer* [2013], *Boon* [2012], and others. *Ezer* [2013] described the significant spatial difference in mean SLR and acceleration between stations north and south of Cape Hatteras, apparently a dynamic response related to the separation point of the GS from the coast. However, the spatial pattern of flooding along the coast may be more complex, because in additional to the spatial pattern of SLR, variations in tidal range and in the frequency of storms also vary along the coast, as quantified recently by *Zhang and Sheng* [2013].

## 3. Results

### 3.1. Flood Duration and Frequency: Impact of Sea-Level Rise and Tides

Communities prone to flooding often prepare for flood events based on expected water level (relative to, e.g., MHHW) obtained from tide and storm surge models. For example, in a flood-prone neighborhood near downtown Norfolk, high tide is sometimes accompanied by unexplained anomalous high waters that may reach 0.3 m (~1 foot) above MHHW even when there is no local wind events (see section 3.3 for more details). This condition can result in minor tidal flooding that can cause what is referred to as "nuisance flooding." When an additional weather front passes the region during high tide, water level may reach 0.6 m (~2 feet) above MHHW and more streets will be flooded. During a major tropical storm, nor'easter or hurricane, water level could reach over 0.9 m (~3 feet) above MHHW (Figure 3) and several blocks of city streets from the water front will be completely under water. In the latter case, flood gates in the downtown area of the city and in highway tunnels would be closed. Therefore, the same statistics of annual flooding time that has been used to characterize floods and plan mitigation strategies in Norfolk [*Atkinson et al*., 2013] have been extended here to other locations; examples are shown in Figures 4a–4g and the results for all the 11 locations are listed in Table 1. The terms "minor," "moderate," and "major" flooding events refer here to 0.3, 0.6, and 0.9 m above MHHW, respectively, though specific locations

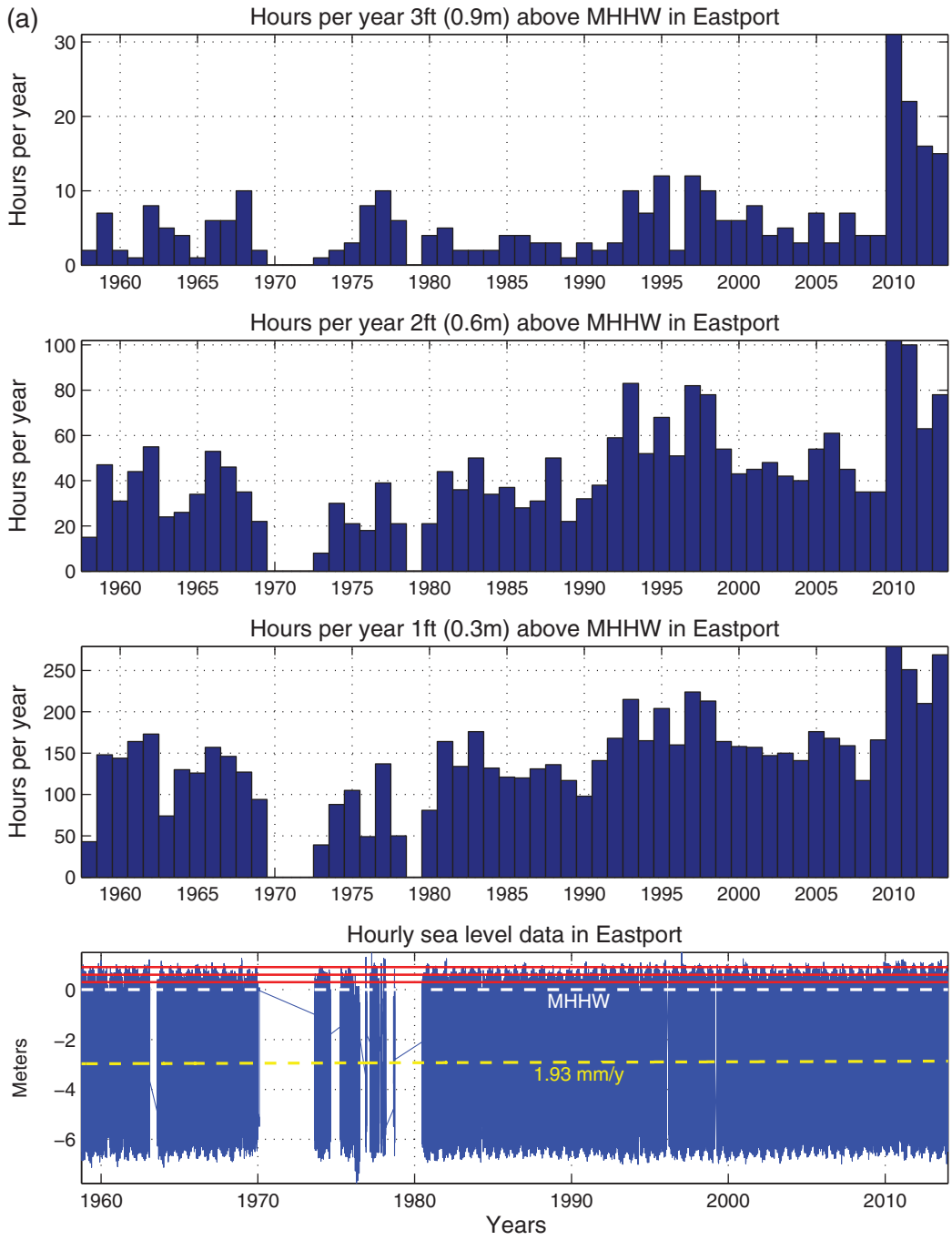


**Figure 4.** (a) Potential flooding statistics for Eastport, ME, in the Gulf of Maine. From bottom to top: (1) hourly sea-level data, and hours per year of water reaching (2) 0.3 m, (3) 0.6 m, and (4) 0.9 m above MHHW (the values in meter are exact, while the values in feet are approximated; the Imperial/U.S. Customary Units are listed because they are used in weather reports and flood risk assessment in the United States). Yellow, white, and red lines in (1) indicate linear SLR trend, MHHW, and the three flood lines, respectively. (b) Same as Figure 4a, but for Portland, ME, in the Gulf of Maine. (c) Same as Figure 4a, but for Battery station, New York, NY. (d) Same as Figure 4a, but for Sewells Point, Norfolk, VA, in the lower Chesapeake Bay. (e) Same as Figure 4a, but for Wilmington, NC. The station is located in the Cape Fear River, which is connected to the South Atlantic Bight. (f) Same as Figure 4a, but for Charleston, SC, in the South Atlantic Bight. (g) Same as Figure 4a, but for Key West, FL.

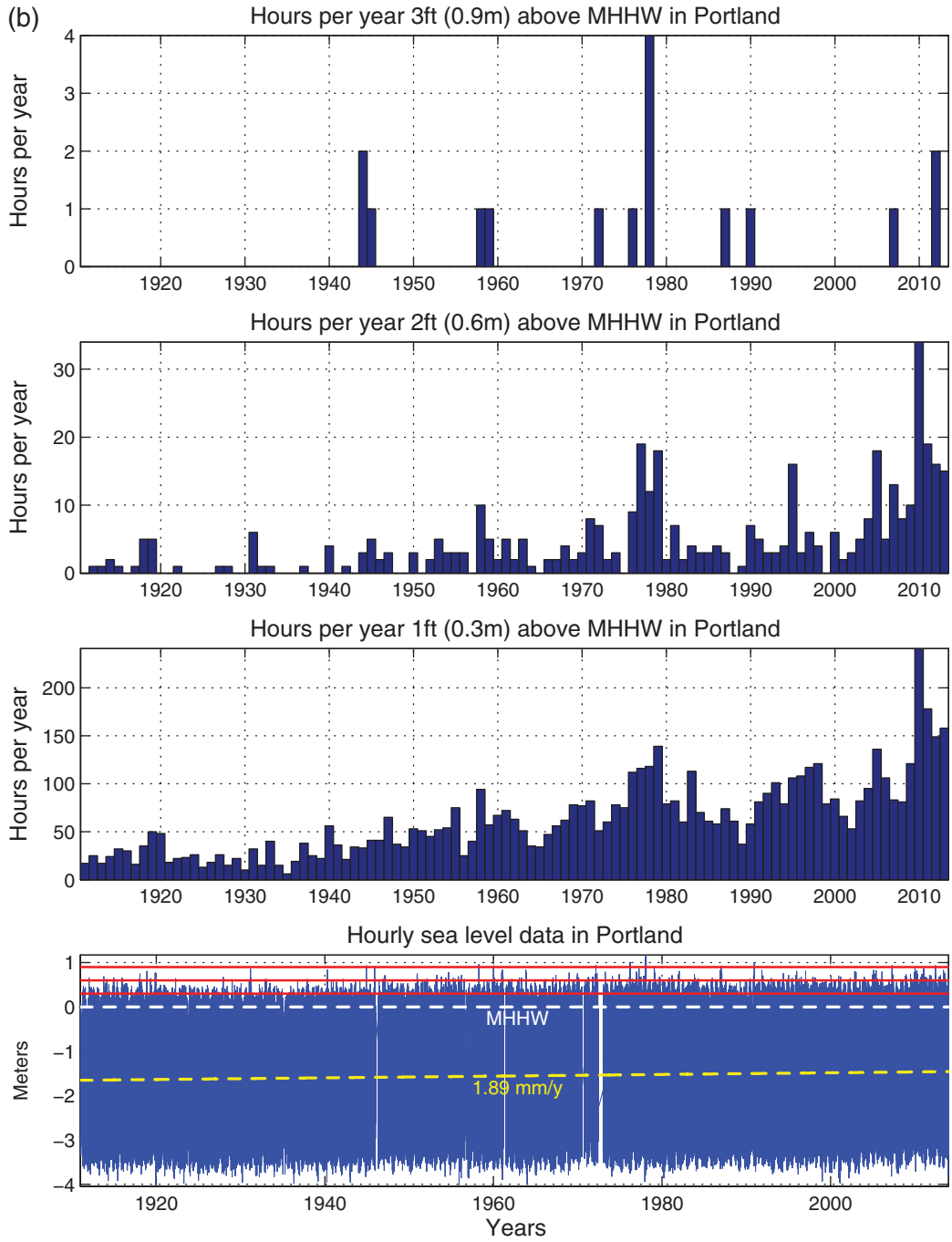


**Figure 4.** (continued)

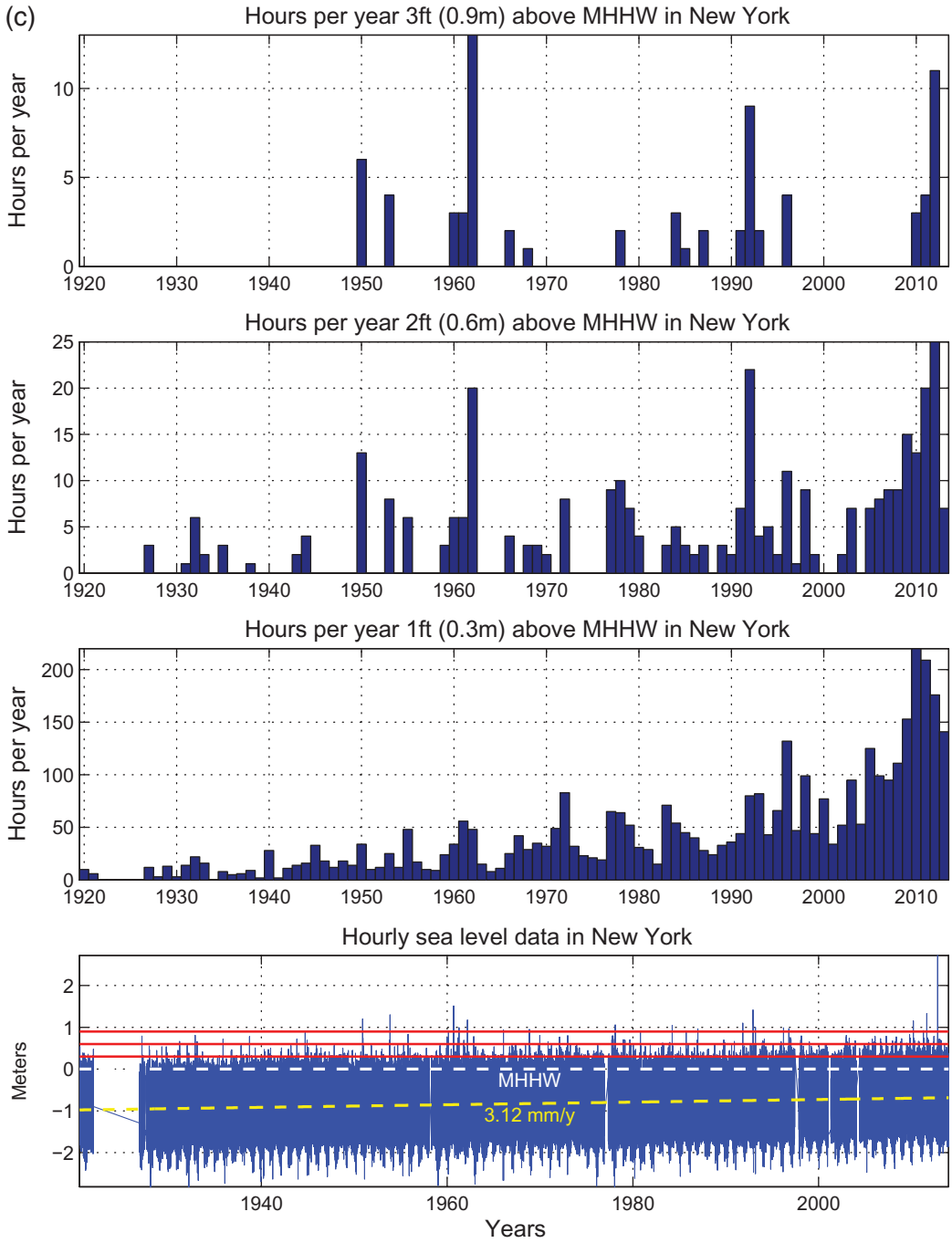


**Figure 4.** (continued)

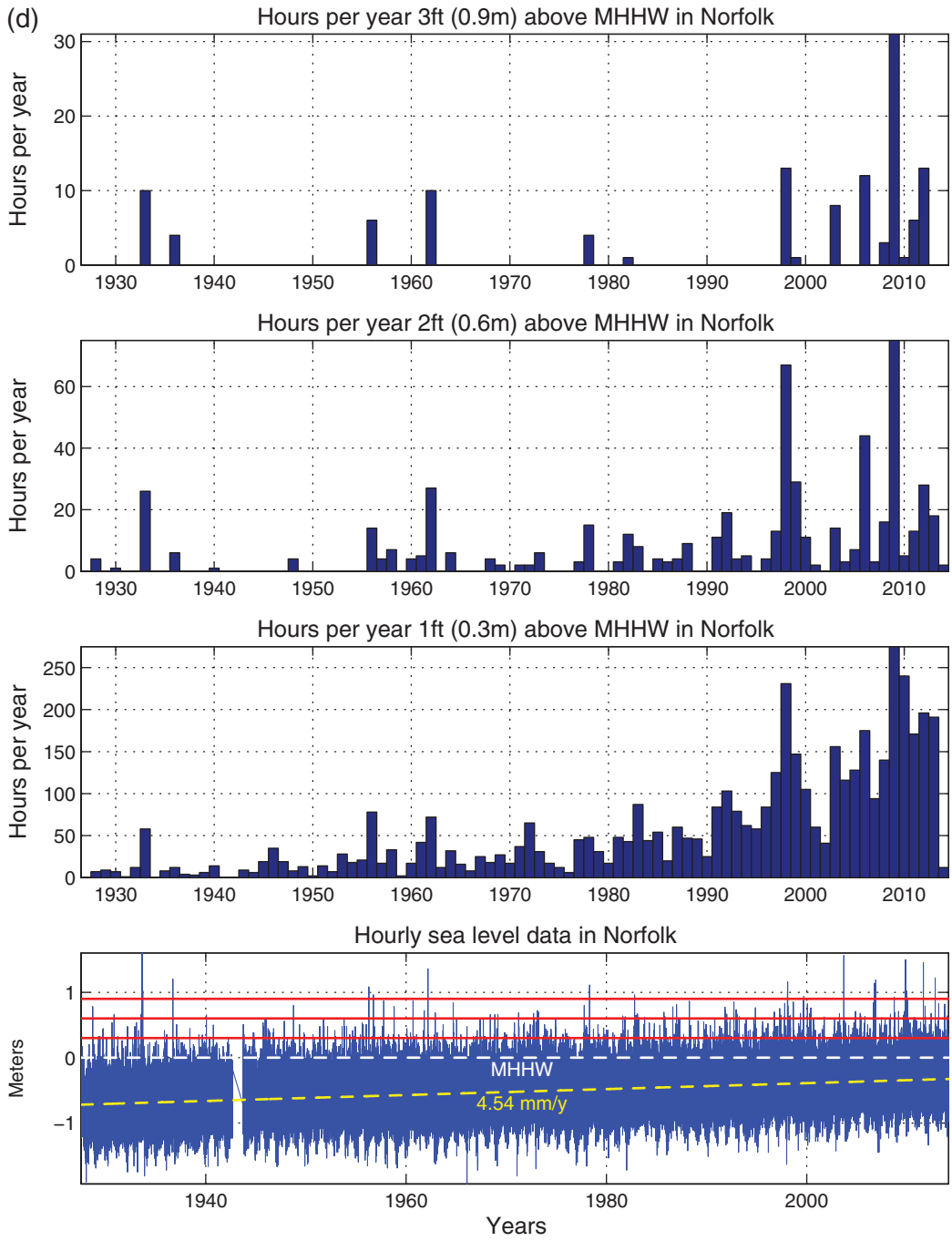


**Figure 4.** (continued)

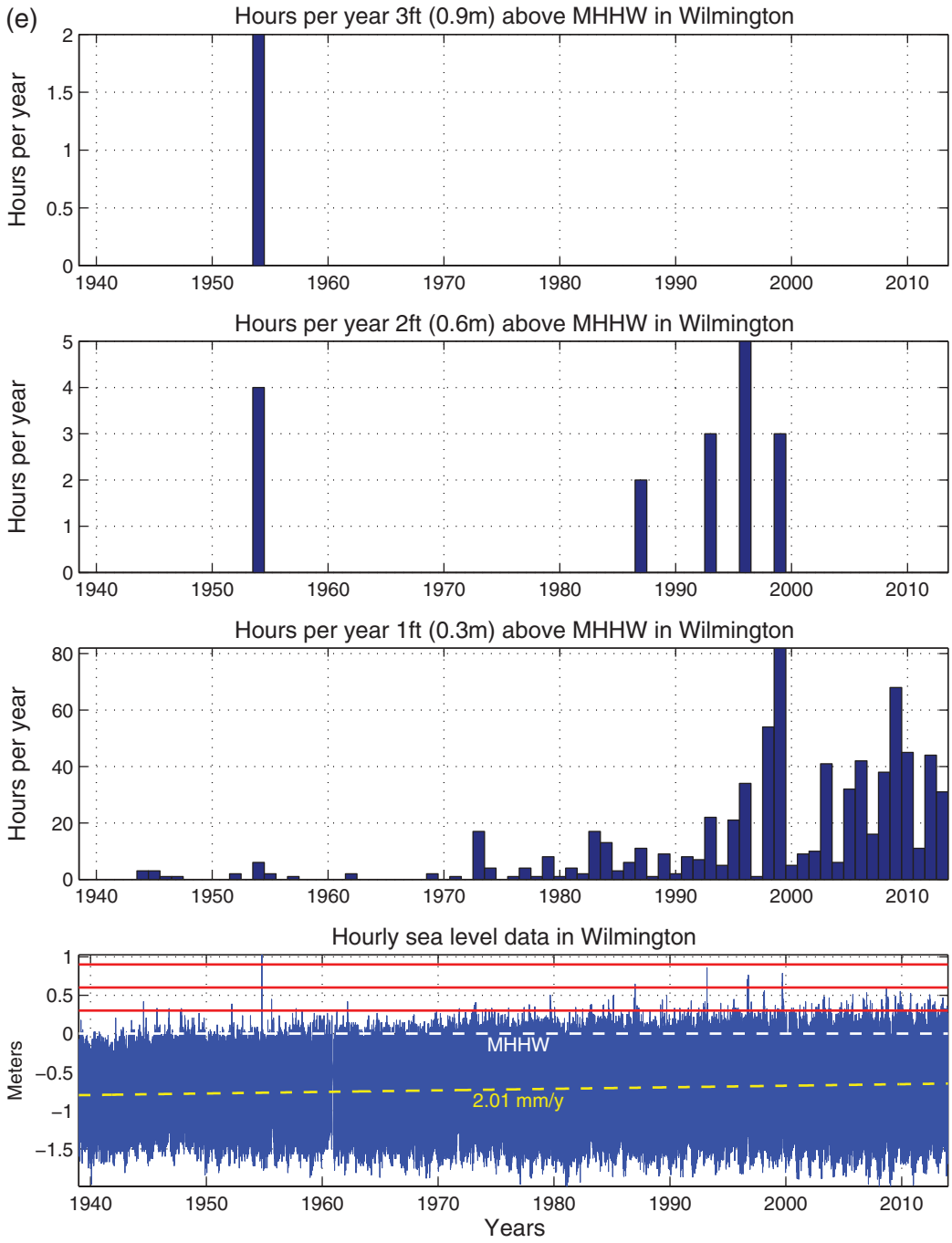


**Figure 4.** (continued)

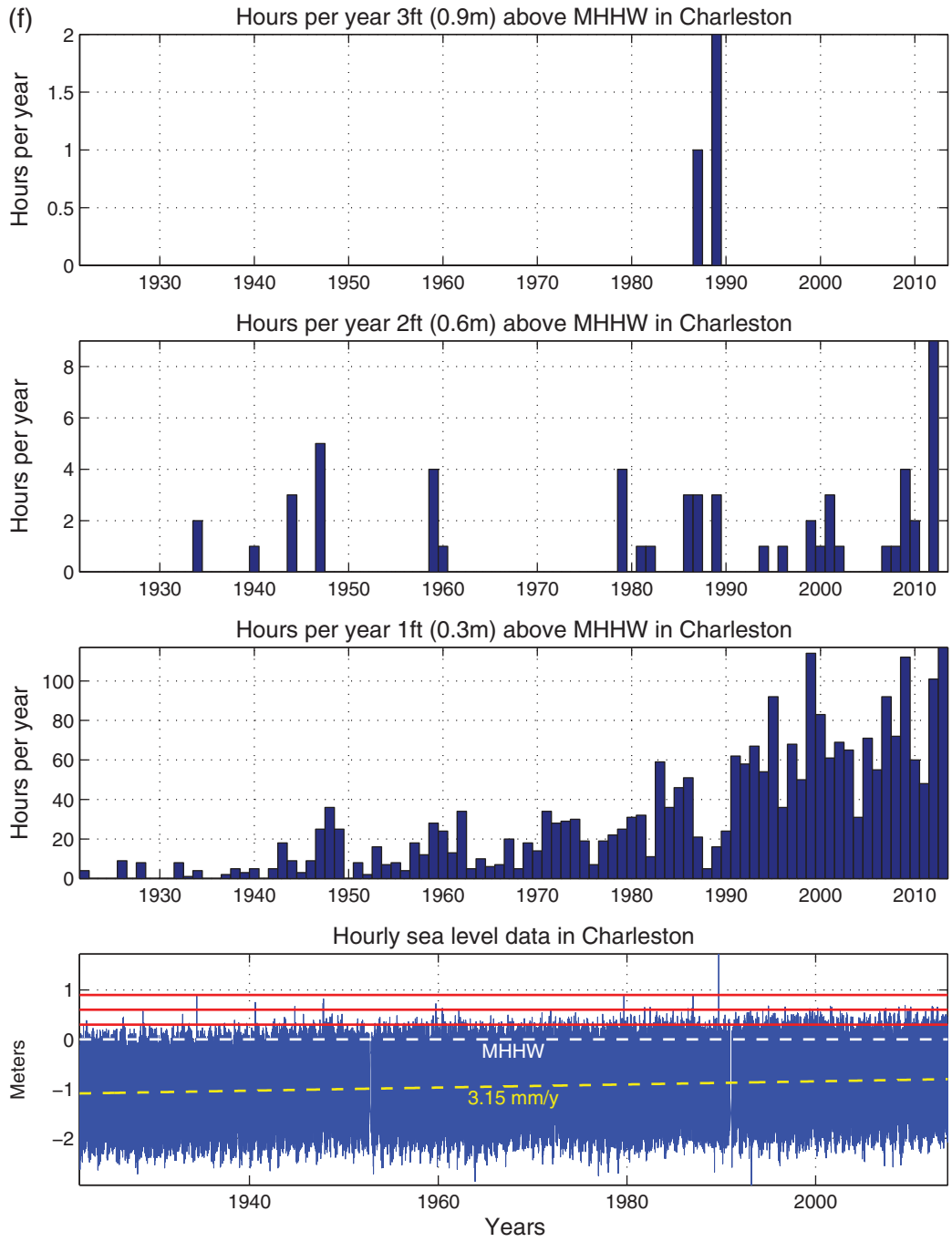


**Figure 4.** (continued)

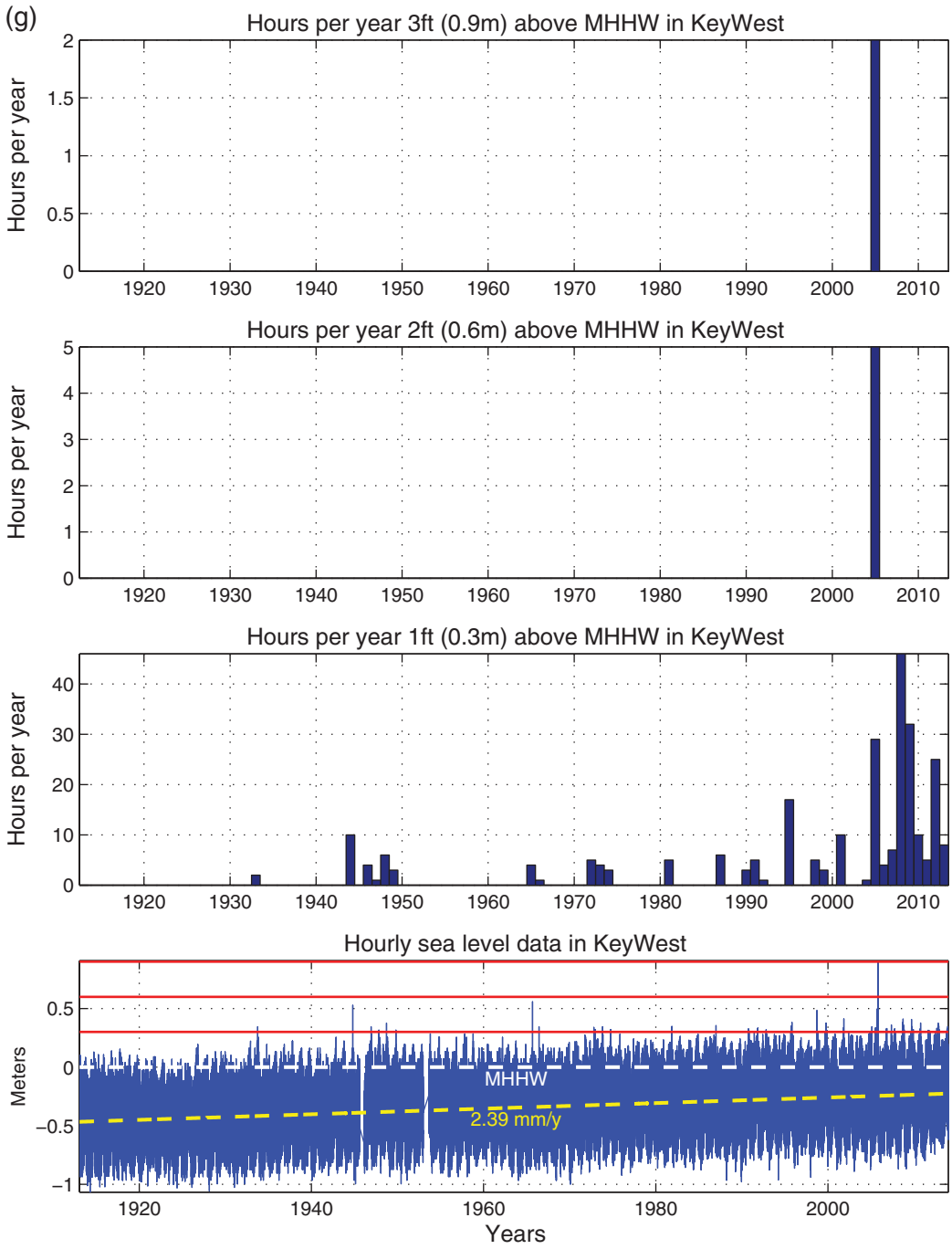


**Figure 4.** (continued)

may have different coastal slopes, height of streets above water, or some protection measures (e.g., flood walls), so that the actual flood risk may be different.

The impact of tidal range on potential flooding can be seen, for example, in the difference between Eastport (Figure 4a) and Portland (Figure 4b). The two stations located in the same region, the Gulf of Maine, have similar tidal modulation (Neap/Spring tide relation) and similar SLR, but the tidal range is almost twice as large in Eastport than it is in Portland (Table 1), resulting in 2–10 times longer flood duration in Eastport than that in Portland. It is to be noted that tidal range by itself may not predict the exceedance probability very well if tidal modulation is different, as demonstrated, for example, by some Australian stations [*Hunter*, 2012]. The potential for minor, moderate, or major floods in Eastport is dominated by the high tide, and between 1958 and 2009 the increase in flooding due to SLR is relatively small. However, in every year since 2010 major floods (top panel of Figure 4a) are larger than in any year before 2010. This may relate to the unusual warming north of the GS that started around 2004 and affected the lobster fishery in the Gulf of Main [*Mills et al*., 2013]. In Portland (Figure 4b) and Boston (not shown), on the other hand, significant increase in minor and moderate flooding due to SLR is more visible, but extreme sea level (major flooding) is rare and shows only decadal variations with no apparent gradual increase. In the Mid-Atlantic region, New York (Figure 4c), Atlantic City and Lewes (not shown), and Norfolk (Figure 4d), dramatic increase in minor and moderate flooding is seen, which is consistent with the high SLR and recent acceleration of SLR in this region [*Boon*, 2012; *Sallenger et al*., 2012; *Ezer*, 2013; *Ezer et al*., 2013; *Kopp*, 2013]. In Norfolk, for example (Figure 4d), years with more than 50 h of minor flooding were very rare until the 1980s (four times in over 50 years) and only happened when nor'easters or hurricanes passed the region. However, over the past 20 years, minor flooding of 50–250 h $yr^{-1}$ became commonplace. In the South Atlantic Bight, the pattern of flooding is quite different than that of the Mid-Atlantic region, because relative coastal SLR associated with land subsidence [term SUB in equation (1)] is not as large, and SLR acceleration is smaller than that in the Mid-Atlantic coastal region [*Boon*, 2012; *Ezer*, 2013]. In Wilmington, there appears to be a significant increase in minor flooding after the 1980s, but it is attributed to an increase in tidal range (bottom panel of Figure 4e) and not due to SLR alone. The tidal station is located in the Cape Fear River; the river has seen continuous sediment filling and several cycles of dredging over the years, which apparently changed the tidal dynamics. In Wilmington (Figure 4e) and Charleston (Figure 4f), major floods are rare and happened only during a couple of hurricanes. Key West, with its small tidal range (Figure 4g), experienced an increase in minor flooding only over the past decade, and almost no major floods except a single year, 2005 (when hurricanes Katrina and Wilma passed nearby).

Figure 5 summarizes the minor flooding (0.3 m above MHHW) hours at the 11 locations; the averaged annual flooding is calculated for three periods: (1) before 1971, (2) 1971–1990, and (3) 1991–2013. While all stations show significant increase in flooding from the 1970s to the 1990s and 2000s, an apparent spatial pattern emerges from this comparison. Three locations are clearly distinct from the general pattern: the northernmost location, Eastport, has such a large tidal range that it is the only location with high minor floods (over 40 h) even before 1971, whereas the southernmost point, Key West, has very minimal floods throughout the record. Wilmington, just south of Cape Hatteras, also has an unusual pattern, with almost no flooding until 1990, but a large increase of 10-fold in recent years due to local sand fill and dredging that caused an increased tidal range, as discussed before. There is a significant increase in flooding at all locations, which is typically ~200%–600% after the 1990s relative to the floods experienced before the 1970s. The question is "Is there a consistent acceleration in flooding?" The acceleration in minor flooding is estimated by

$$\mathrm{ACC}\ \left(\mathrm{h\ yr^{-2}}\right) = \frac{\frac{(T3-T2)}{(Y3-Y2)} - \frac{(T2-T1)}{(Y2-Y1)}}{(Y3-Y1)/2}. \tag{3}$$

$Y1$, $Y2$, and $Y3$ are the years in the middle of the three periods, from the beginning of the record to 1970, from 1971 to 1990, and from 1991 to 2013, respectively, and $T1$, $T2$, and $T3$ are the average annual flooding hours for the three periods. All the stations show positive acceleration (Table 1) and a distinct pattern. Excluding the northernmost and southernmost stations, acceleration in flooding increases gradually as one moves south from Portland (ACC ~ 0.01 h $yr^{-2}$) to Lewes and Norfolk (ACC ~ 0.15 h $yr^{-2}$), and then from Wilmington (ACC ~ 0.04 h $yr^{-2}$) to Pulaski (ACC ~ 0.08 h $yr^{-2}$). The change in the acceleration at Cape Hatteras and the general pattern of ACC closely resembles the SLR acceleration pattern found

10.1002/2014EF000252

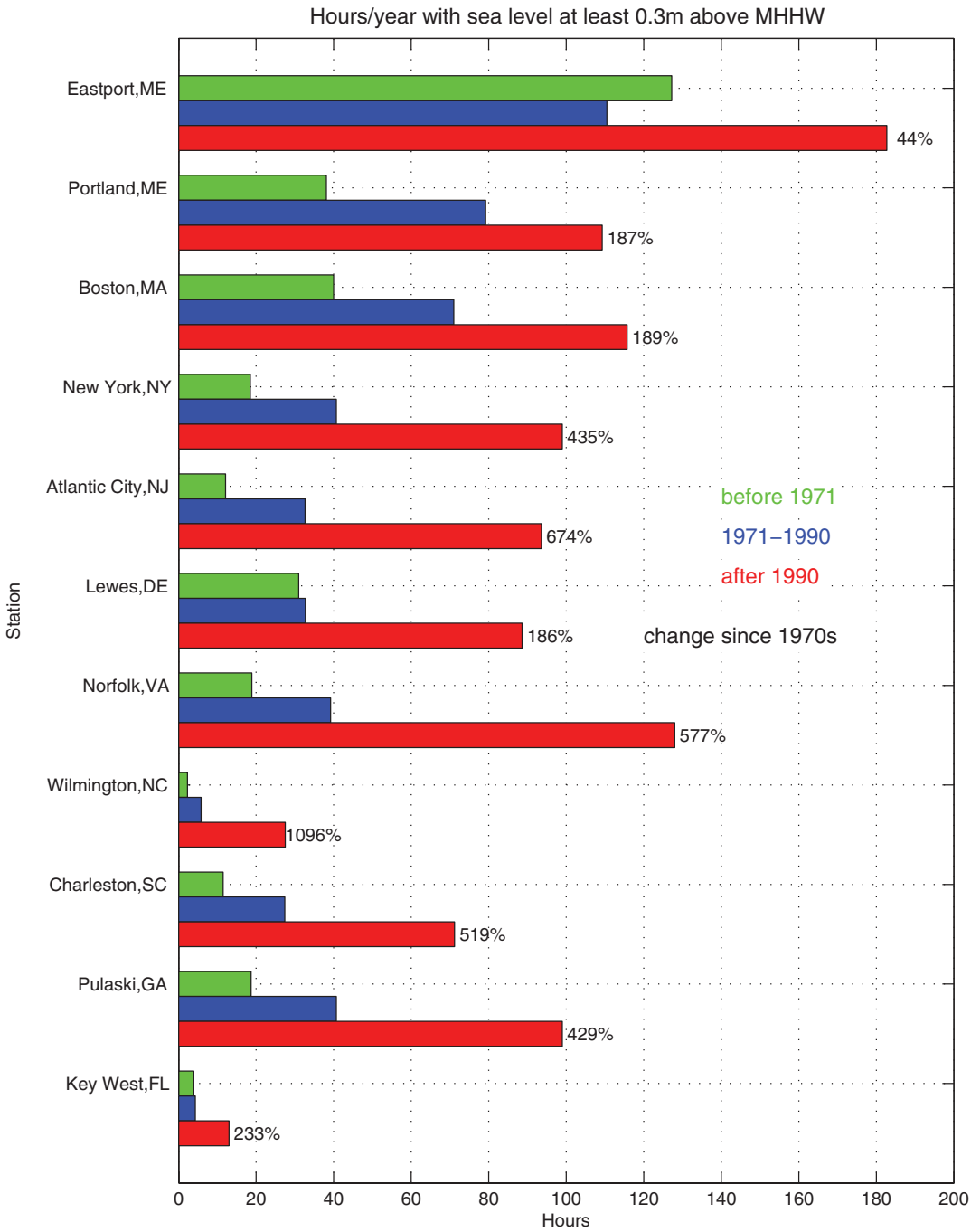


**Figure 5.** Summary of the mean number of hours per year of water level of at least 0.3 m above MHHW. Green, blue, and red bars are averages over three different periods, before 1971, 1971–1990, and 1991–2013, respectively. The percentage increase in potential minor flooding from the first to the third period is indicated for each station.

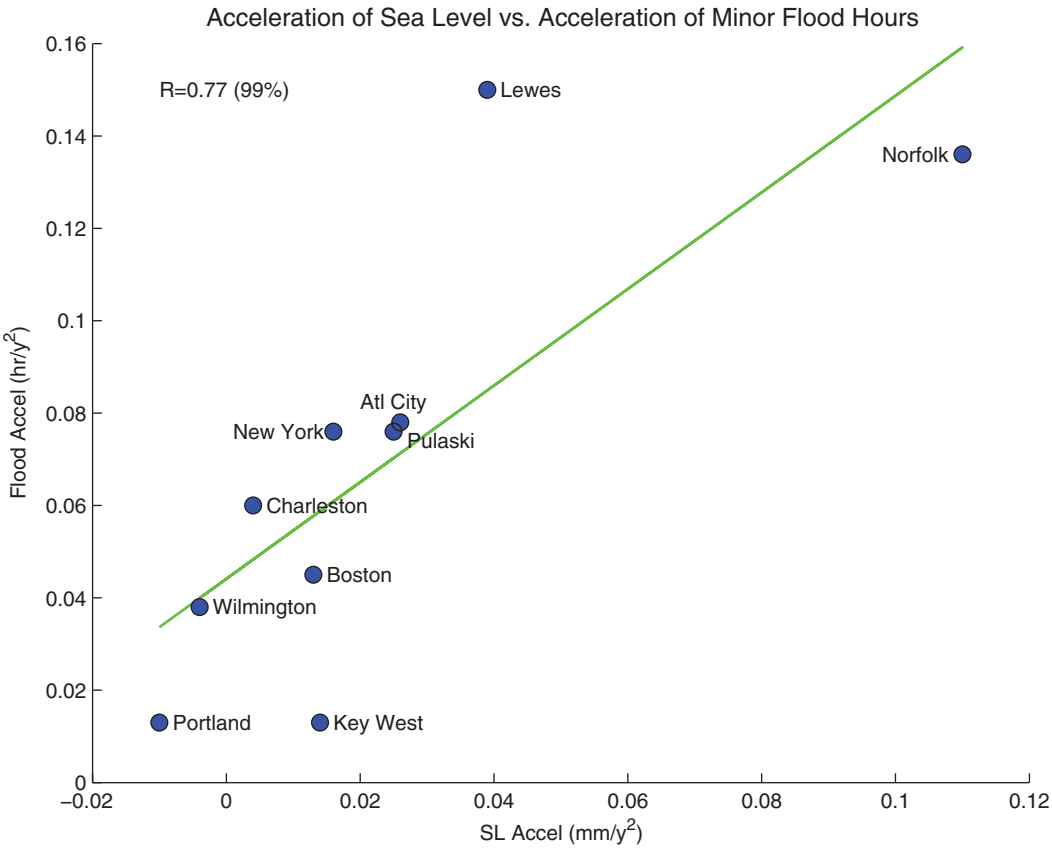


**Figure 6.** Acceleration in SLR [in mm $yr^{-2}$, from *Ezer*, 2013] versus acceleration in minor flooding (in annual flood hours of 0.3 m over MHHW per year); see text for details of the calculations. The data from Eastport are omitted owing to its unusual high tide relative to other stations (Figure 5). The linear regression line (in green), the correlation coefficient, and the confidence level of the correlation are indicated.

by *Ezer* [2013]. Although acceleration in SLR is not necessarily precondition for acceleration in flooding, the similarity in the pattern of spatial variations between acceleration in SLR and flooding suggests that ocean dynamics [i.e., term LOC in equation (1)] may play a role in causing the differences between the Mid-Atlantic Bight north of Cape Hatteras and the South Atlantic Bight south of Cape Hatteras. Figure 6 compares the acceleration in minor flooding (ACC) with the acceleration in sea level, calculated by *Ezer* [2013]; the latter uses an empirical mode decomposition (EMD) method to separate a nonlinear trend from oscillating modes [see *Ezer and Corlett*, 2012 for details]. Data at Eastport were omitted in Figure 6 owing to its unusual high tide that obscures the results. Results show that accelerations in sea level and in floods are significantly correlated ($R = 0.77$, confidence level > 99%). The largest acceleration in both sea level and flood duration is at Norfolk, VA, and Lewes, DE, the closest locations downstream from the separation point of the GS at Cape Hatteras. The locations with the lowest flood acceleration are those farthest away from Cape Hatteras in both directions (Portland in the north and Key West in the south).

The contributions of tides and SLR to (minor) flooding are shown in Figure 7 (excluding data from Wilmington due to varying tidal range). Before 1990, flooding period was highly correlated with the tidal range (correlation coefficient $R > 0.9$ and statistical confidence > 99.9%) and only small differences are seen between the period before 1971 and 1971–1990. After 1990 SLR appears to play an additional role, so the correlation between tidal range and flooding is somewhat smaller ($R = 0.77$, though still significant at 99% level). The fact that all three lines in Figure 7 have almost the same slope indicates that tidal contribution to flooding is quite linear and predictable. The average increase in minor flooding is ~20 h $yr^{-1}$ between the beginning of the records to 1970 and 1971–1990, but ~50 h $yr^{-1}$ between 1971–1990 and 1991–2013.

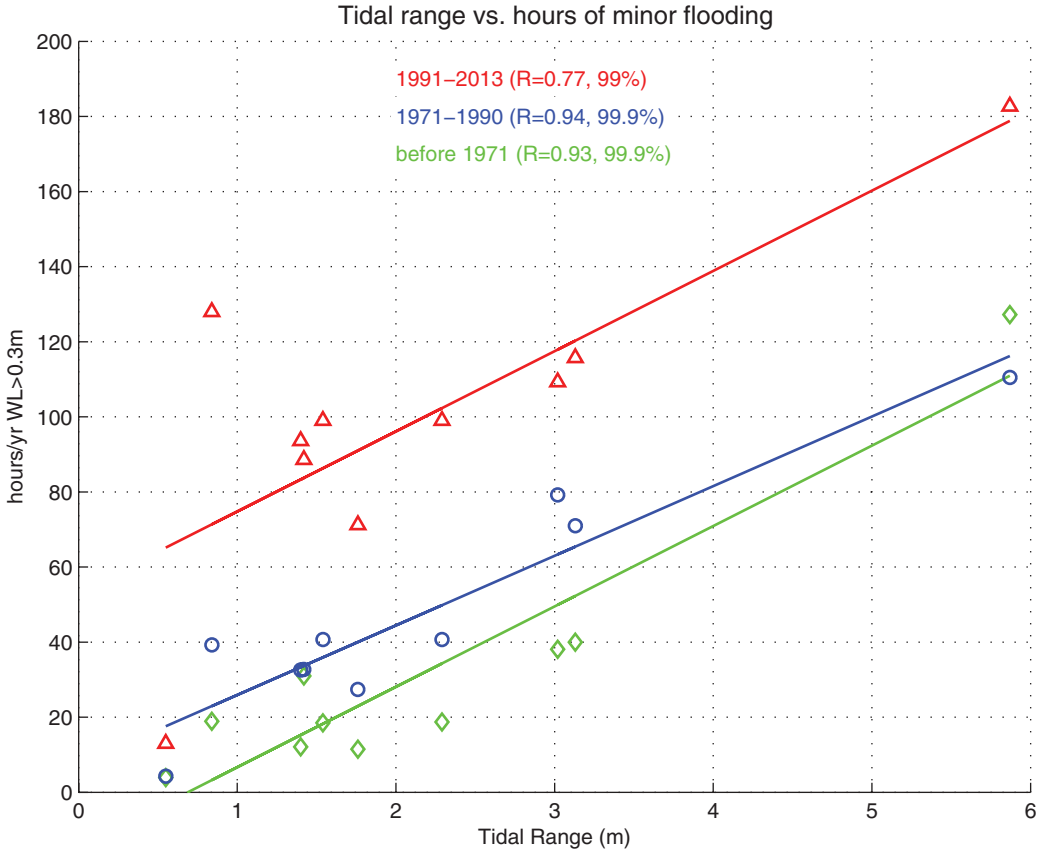


**Figure 7.** The impact of tidal range on potential minor flooding (0.3 m above MHHW). The green, blue, and red markers and line fit represent the same three periods as in Figure 5. The linear correlation coefficients and statistical confidence level are indicated.

### 3.2. Extreme Sea-Level Events and the Impact of the North Atlantic Oscillations

Extreme storm surge events (defined here at 0.9 m over MHHW) are relatively rare and are related to hurricanes or intense storms (except where tides are very large, such as in Eastport). A storm such as Hurricane Sandy caused more floods in 2012 than a storm with similar strength 100 years ago when sea level was lower (assuming both hit at the same tidal stage) [*Kemp and Horton*, 2013]. However, predicting the frequency of big storms and the location they hit the coast may be difficult and depend on many factors, such as variations in weather and climate over the continental United States and conditions over the Atlantic Ocean. Figures 3 and 4 (and the other stations not shown) indicate that extreme sea-level events in the Mid-Atlantic region have some decadal-like variations rather than a gradual increase as seen in minor and moderate flooding events, suggesting a modulation by large-scale ocean-atmosphere patterns.

One of the most widely used patterns that affect decadal and multidecadal variations in the Atlantic region is the North Atlantic Oscillation (NAO) index [*Hurrell*, 1995], representing north-south dipole of pressure anomalies over the North Atlantic Ocean. The NAO is associated with changes in the intensity and location of the jet stream and storm track, as well as changes in temperature and precipitation patterns. For example, strong positive phases of the NAO tend to be associated with warmer temperatures in the eastern United States. The NAO may also be connected to long-term variations in sea level and the transport of the GS [*Ezer et al*., 2013]. An extreme storm surge event is defined here as a year with at least one event with water level reaching at least 0.9 m above MHHW (i.e., a nonzero bar in the upper panels of Figure 4). While it is possible that a single storm moving along the coast may cause extreme events at more than one location, they are considered here as separate events, because we attempt to characterize the total impact of storms on the coast. An index of the average number per year of extreme storm events hitting somewhere along the coast for each 5 year period is shown in Figure 8 (green line) and compared with 5 year averages of the NAO index (blue line). Only stations with at least two extreme

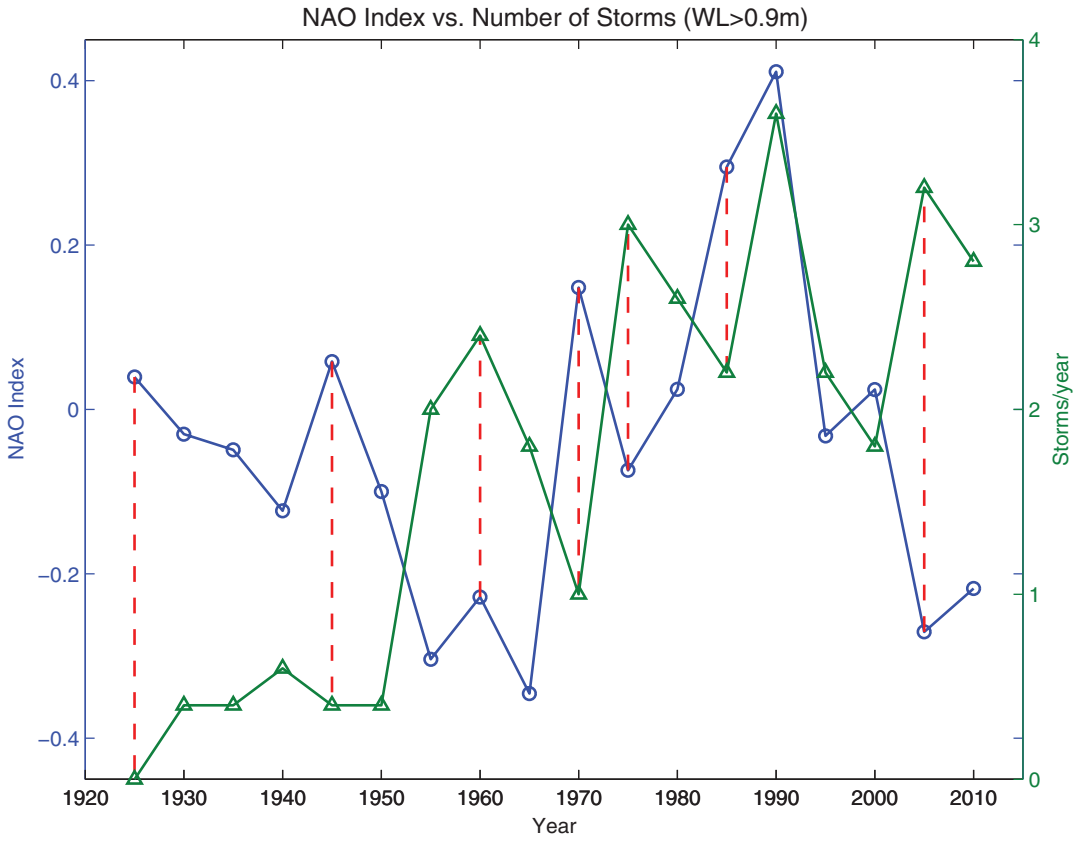


**Figure 8.** The number of extreme storm surge events versus the North Atlantic Oscillation (NAO) index. Green line and axis on the right: index of "high-water storm events" calculated by the average number of storm surges per year for each 5 year period. A storm event is defined as a year in which water level reached 0.9 m over MHHW at least once at any station (i.e., each nonzero bar in the top panels of Figures 4a–4e is considered as a "storm event"). Multiple storms hitting the same location on the same year are counted once, but impact of same storm at two different locations is considered as two impacts. Blue line and axis on the left: 5 year averaged NAO index. Each marker is located at the beginning of a 5 year period. The vertical red dashed lines indicate times where high/low peaks in storm events coincide with low/high peaks in the NAO index.

events were included. The small number of events does not allow calculating statistical significance, but qualitatively there appear to be interesting relations between NAO and extreme events. The average number of extreme storm surge events per year generally increased from ~0.5 before 1950 to ~3.5 in 1990; at the same time the NAO shows an upward trend as well; *Hurrell* [1995] and others described this multi-decadal shift in the NAO. An increase in storminess [*Dawson et al*., 2002] and warmer temperatures along the U.S. coast associated with more positive NAO [*Mills et al*., 2013] may relate to this trend, though more research on this possibility is needed, which is beyond the scope of this study. During the time between the 1970s and 1990s the subpolar region also experienced an increase in sea level and weakening circulation [*Hakkinen and Rhines*, 2004], which may have weakened the AMOC and the GS transports [*Ezer et al*., 2013]. An interesting result is that between 1950 and 2010 there is an oscillation in the number of extreme events with a period of about 15 years (significant peaks in extreme events in 1960–1965, 1975–1980, 1990–1995, and 2005–2010). Those variations show that minima and maxima and extreme events are anticorrelates with peaks in the NAO (seven such cases are indicated by the vertical red bars in Figure 8), so more storms appear to be expected during a period when NAO reached a local minimum. These variations could relate to wind-driven decadal variations in the Atlantic Ocean circulation and GS transport [which was found to be anticorrelated with NAO variations; *Ezer et al*., 2013]. In any case, while SLR contributes to the damage caused by extreme storm surge events, it does not appear to explain the decadal pattern of extreme flooding events, so one needs to also consider large-scale atmosphere-ocean patterns.

### 3.3. Minor Short-Term Flooding and the Impact of the GS

Recent studies suggest a strong connection between long-term variations in the GS and coastal sea level [*Ezer*, 2013; *Ezer et al*., 2013], whereas weakening of the GS reduces the sea-level slope across the

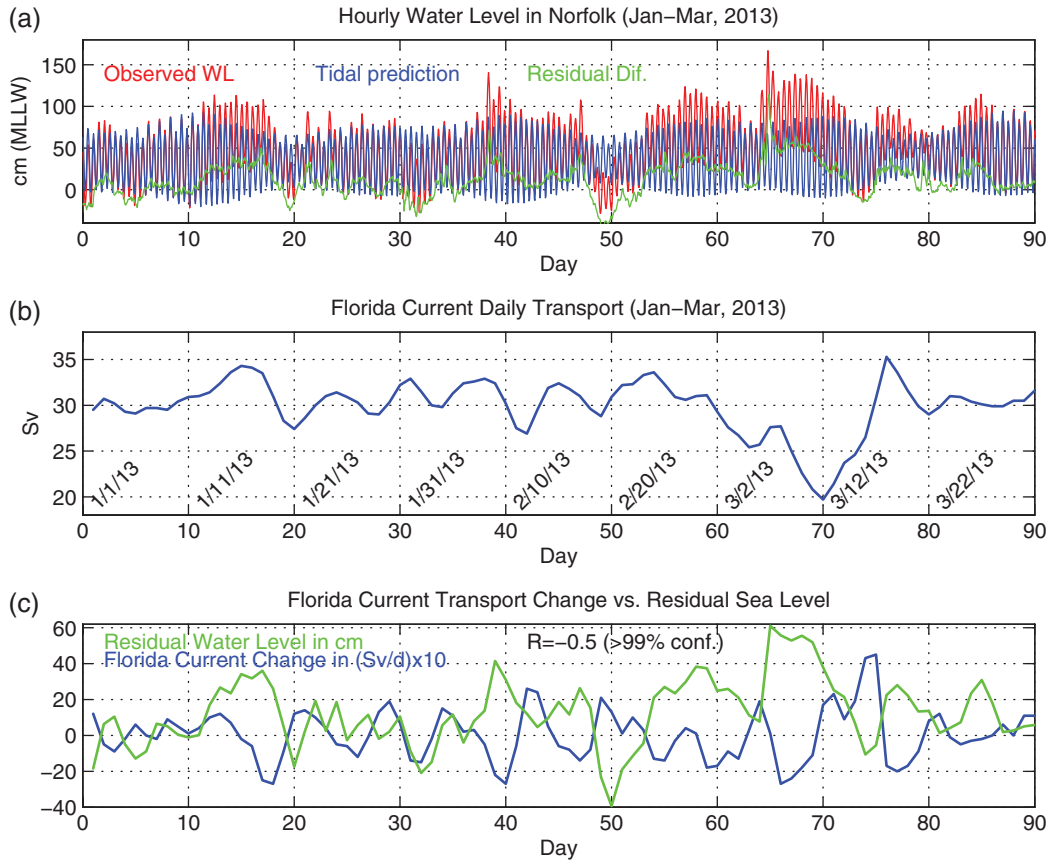


**Figure 9.** (a) Example of hourly water level in Sewells Point, Norfolk, from January to March 2013. Red, blue, and green lines represent observed water level, tidal prediction, and residual (observed-prediction), respectively. (b) Daily Florida Current (FC) transport recorded by the cable data across the Florida Straits. (c) The water level residual anomaly in Norfolk (green; in cm) and the FC transport change (blue; in Sv change per day times $10 = 10^5$ m$^3$ d$^{-1}$); the correlation coefficient and confidence level of the correlation between sea-level anomaly and FC change are indicated.

GS, resulting in lower water level east of the GS and higher water level onshore along the coast. The same studies found that variations in the GS strength, estimated from either satellite altimeter data over the Mid-Atlantic Bight [*Ezer et al*., 2013] or direct observations of the FC transport across the Florida Strait [*Ezer*, 2013], produce similar correlations with decadal variations in coastal sea level. Connections between the GS transport at the Florida Straits and coastal sea level, from Key West to Norfolk, on seasonal timescales, have been suggested as well [*Blaha*, 1984]. High-frequency (e.g., mesoscale or wind-driven) variations in the strength of the GS may also influence high-frequency variations in coastal sea level. For example, a NOAA report [*Sweet et al*., 2009] suggests that unusually high water level along the Mid-Atlantic coast in the summer of 2009 may have been related to a period of weak FC transport. Low-lying cities in the Chesapeake Bay, such as Norfolk, VA, noticed in recent years prolong periods of flooding during high tides when water levels exceed the official NOAA prediction by 0.3–0.5 m, even when there is no storm in the region. Wind-driven numerical models appear to underestimate these events by as much as 0.5 m. Could such events be partly responsible for the increase in frequency of minor flooding events as observed around the Chesapeake Bay? [*Atkinson et al*., 2013; *Boesch et al*., 2013; *Mitchell et al*., 2013]. As an example, Figure 9a shows the hourly tidal prediction and observed water level in Sewells Point, Norfolk, for the first 3 months of 2013. During this period, there were no major storms, but at least six events when the observed water level was at least 20 cm above the NOAA prediction for more than one tidal cycle (causing minor street flooding in downtown Norfolk), and one event of extremely low observed water level of 40 cm below the prediction (day 50). While some of the short (~1 day) anomalies may be due to local wind, there is no atmospheric explanation for high water anomaly that lasts for weeks (e.g., days 55–75). When comparing the water-level anomaly (or residual) to the daily

FC transport [*Baringer et al*., 2013] (Figure 9b), it was found that the change in the transport is highly anticorrelated ($R = -0.5$; significance > 99%) with the water level (Figure 9c). When the FC (i.e., the GS measured at the Florida Strait) is on a weakening trend such as from February 20 to March 12, water level is considerably higher than normal (with only a short break when the FC increased slightly at day 65). *Ezer et al*. [2013] noticed that on decadal scales water level in the Mid-Atlantic coast has higher correlations with *changes* in the GS (after it separated from the coast), then the correlation with the GS strength itself; a simple dynamic balance equations were presented by Ezer et al. to explain this relation. They also show significant correlation on monthly to decadal scales between the FC cable transport upstream of Cape Hatteras and altimeter-derived GS strength downstream of Cape Hatteras. Here it was shown that the same mechanism also works for high-frequency oscillations. The fact that there is no time lag between changes in the FC at 27°N and changes in sea level more than 1000 km farther north indicates that the entire western boundary current may have some coherent variations that are probably driven by Ekman transports associated with variations in the large-scale wind stress over the subtropical gyre [*McCarthy et al*., 2012]. A recent study, using data and models, in fact, supports the hypothesis suggested above; it shows coherent correlation between FC transport and sea level along the GS from south Florida to 40°N and coherent correlation between the FC transport and wind stress over the subtropical gyre [Figure 4 in *Zhao and Johns*, 2014]. If oceanic anomalies in sea level propagate toward the coast by means of fast-moving barotropic waves, the response at the coast would be within hours. More research is needed on this driving mechanism, which is beyond the scope of this paper. However, a practical implication of the finding is the possibility to improve water-level prediction on the coast using GS data from either satellite or the FC cable measurements.

## 4. Summary and Conclusions

Recent findings show an accelerated SLR (hotspot) along the U.S. East Coast north of Cape Hatteras and significant variations of SLR rates along the coast [*Boon*, 2012; *Ezer and Corlett*, 2012; *Sallenger et al*., 2012; *Ezer*, 2013; *Kopp*, 2013]; a potential driver for those may be climate-related changes in the AMOC [*Hakkinen and Rhines*, 2004; *McCarthy et al*., 2012; *Srokosz et al*., 2012; *Smeed et al*., 2013] and its upper branch, the GS [*Ezer et al*., 2013]. But it is not always clear how this information can be used to assess risks and impacts on different coasts and cities vulnerable to flooding [*Nicholls and Cazenave*, 2010; *Cazenave and Cozannet*, 2014]. Therefore, we calculated here a matrix of flood statistics, based on three given water level above a known high tide reference level (representing "minor," "moderate," and "extreme" flood events); this analysis is more easily used for practical purposes of flood mitigation and risk assessment than standard exceedance probability statistics (though the two methods are related). The results show very clearly that the U.S. East Coast (in particular the Mid-Atlantic coastal area north of Cape Hatteras) is a "hotspot of accelerated flooding" and that acceleration in SLR is highly correlated with acceleration in minor flood durations. Minor to moderate flooding increased significantly in the 1990s. Until the 1980s, the increase in flooding was relatively moderate, and flooding was, in most cases, associated with particular storm events. However, in recent years, flooding became more common and even a small weather front or anomaly related to offshore currents change can cause flooding over several tidal cycles. The result is acceleration in flooding durations, with larger increase in flooding along the coasts of the lower Mid-Atlantic Bight, where SLR acceleration is also larger. An interesting result was that extreme storm surge events appear to be correlated with decadal and multidecadal variations of the NAO, in addition to the general increase in flooding due to SLR. It was found that decadal oscillations (of ~15 year period) in the number of extreme storm surge events are anticorrelated with decadal variations in the NAO; the results are consistent with the mechanism involved wind-driven oscillations in the Atlantic Ocean circulation and the GS [*Ezer*, 1999, 2001; *Ezer et al*., 2013].

What are the implications of these results with respect to flood risks due to future SLR? The average recurrence interval is expected to change, so in Norfolk, for example, a flood with a 80 year return level (defined by an annual exceedance probability of 1/80) today is expected to occur in average every ~40 years if sea level would rise by 0.1 m; by 2050 when sea level in Norfolk is expected to rise by ~0.5 m [*Boon*, 2012; *Ezer and Corlett*, 2012] such flood level will be expected to occur every ~6 years (based on our calculations, not shown, and statistics provided by NOAA). The increase in the impact of storm surges due to rising seas and potentially due to slowing down of the GS will result in an increase in flood durations, as demonstrated

here. The main goal of this study was to provide information on flood statistics, spatial variations, and the various forcing components involved, in the hope that such information will be useful for improving flood predictions and for planning mitigation and adaptation strategies in flood-prone regions such as the Hampton Roads area (where the authors reside).

**Acknowledgments**
Old Dominion University's Climate Change and Sea Level Rise Initiative (CCSLRI) as well the Center for Coastal Physical Oceanography (CCPO) provided partial support for this study. John Hunter and an anonymous reviewer are thanked for providing many useful suggestions that greatly improved the paper. Access to all the hourly tide gauge data is available from http://opendap.co-ops.nos.noaa.gov/dods/IOOS/ and the Matlab-based codes to plot all figures are available on request from tezer@odu.edu. The NAO index data can be obtained from http://climatedataguide.ucar.edu.

## References

Atkinson, L. P., T. Ezer, and E. Smith (2013), Sea level rise and flooding risk in Virginia, *Sea Grant Law Policy J.*, *5*(2), 3–14.
Baringer, M. O., et al. (2013), Meridional overturning circulation and heat transport observations in the Atlantic Ocean [in "State of the Climate in 2012"], *Bull. Am. Meteorol. Soc.*, *94*(8), S65–S68.
Blaha, J. P. (1984), Fluctuations of monthly sea level as related to the intensity of the Gulf Stream from Key West to Norfolk, *J. Geophys. Res. Oceans*, *89*(C5), 8033–8042, doi:10.1029/JC089iC05p08033.
Boesch, D. F., L. P. Atkinson, W. C. Boicourt, J. D. Boon, D. R. Cahoon, R. A. Dalrymple, T. Ezer, B. P. Horton, Z. P. Johnson, R. E. Kopp, M. Li, R. H. Moss, A. Parris, and C. K. Sommerfield (2013), Updating Maryland's sea-level rise projections, *Special Report of the Scientific and Technical Working Group to the Maryland Climate Change Commission*, 22 pp., Univ. of Md. Cent. for Environ. Sci., Cambridge, Md.
Boon, J. D. (2012), Evidence of sea level acceleration at U.S. and Canadian tide stations, Atlantic coast, North America, *J. Coast. Res.*, *28*(6), 1437–1445, doi:10.2112/jcoastres-d-12-00102.1.
Boon, J. D., J. M. Brubaker, and D. R. Forrest (2010), Chesapeake Bay land subsidence and sea level change, in *App. Mar. Sci. and Ocean Eng., Rep. No. 425*, Va. Inst. of Marine Sci., Gloucester Point, Va.
Cazenave, A., and G. L. Cozannet (2014), Sea level rise and its coastal impacts, *Earth's Future*, *2*, 15–34, doi:10.1002/2013EF000188.
Church, J. A., and N. J. White (2011), Sea-level rise from the late 19th to the early 21st century, *Surv. Geophys.*, *32*, 585–602, doi:10.1007/s10712-011-9119-1.
Dawson, A. G., et al. (2002), Complex North Atlantic Oscillation (NAO) index signal of historic North Atlantic storm-track changes, *Holocene*, *12*(3), 363–369.
Ezer, T. (1999), Decadal variabilities of the upper layers of the subtropical North Atlantic: An ocean model study, *J. Phys. Oceanogr.*, *29*(12), 3111–3124.
Ezer, T. (2001), Can long-term variability in the Gulf Stream transport be inferred from sea level?, *Geophys. Res. Lett.*, *28*(6), 1031–1034, doi:10.1029/2000GL011640.
Ezer, T. (2013), Sea level rise, spatially uneven and temporally unsteady: Why the U.S. East Coast, the global tide gauge record, and the global altimeter data show different trends, *Geophys. Res. Lett.*, *40*, 5439–5444, doi:10.1002/2013GL057952.
Ezer, T., and W. B. Corlett (2012), Is sea level rise accelerating in the Chesapeake Bay? A demonstration of a novel new approach for analyzing sea level data, *Geophys. Res. Lett.*, *39*, L19605, doi:10.1029/2012GL053435.
Ezer, T., L. P. Atkinson, W. B. Corlett, and J. L. Blanco (2013), Gulf Stream's induced sea level rise and variability along the U.S. mid-Atlantic coast, *J. Geophys. Res.*, *118*, 685–697, doi:10.1002/JGRC.20091.
Haigh, I. D., T. Wahl, E. J. Rohling, R. M. Price, C. B. Battiaratchi, F. M. Calafat, and S. Dangendorf (2014), Timescales for detecting a significant acceleration in sea level rise, *Nat. Commun.*, *5*, 36355, doi:10.1038/ncomms4635.
Hakkinen, S., and P. B. Rhines (2004), Decline of subpolar North Atlantic circulation during the 1990s, *Science*, *304*, 555–559.
Hunter, J. (2010), Estimating sea-level extremes under conditions of uncertain sea-level rise, *Clim. Change*, *99*, 331–350, doi:10.1007/s10584-009-9671-6.
Hunter, J. (2012), A simple technique for estimating an allowance for uncertain sea-level rise, *Clim. Change*, *113*, 239–252, doi:10.1007/s10584-011-0332-1.
Hurrell, J. W. (1995), Decadal trends in the North Atlantic oscillation, *Science*, *269*, 676–679.
Kemp, A. C., and B. Horton (2013), Contribution of relative sea-level rise to historical hurricane flooding in New York City, *J. Quat. Sci.*, *28*(6), 537–541, doi:10.1002/jqs.2653.
Kleinosky, L. R., B. Yarnal, and A. Fisher (2007), Vulnerability of Hampton Roads. Virginia to storm-surge flooding and sea-level rise, *Nat. Hazards*, *40*(1), 43–70, doi:10.1007/s11069-006-0004-z.
Kopp, R. E. (2013), Does the mid-Atlantic United States sea-level acceleration hot spot reflect ocean dynamic variability?, *Geophys. Res. Lett.*, *40*, 3981–3985, doi:10.1002/GRL.50781.
Levermann, A., A. Griesel, M. Hofmann, M. Montoya, and S. Rahmstorf (2005), Dynamic sea level changes following changes in the thermohaline circulation, *Clim. Dyn.*, *24*(4), 347–354.
McCarthy, G., E. Frejka-Williams, W. E. Johns, M. O. Baringer, C. S. Meinen, H. L. Bryden, D. Rayner, A. Duchez, C. Roberts, and S. A. Cunningham (2012), Observed interannual variability of the Atlantic Meridional Overturning Circulation at 26.5°N, *Geophys. Res. Lett.*, *39*, L19609, doi:10.1029/2012GL052933.
Mills, K. E., et al. (2013), Fisheries management in a changing climate lessons from the 2012 ocean heat wave in the Northwest Atlantic, *Oceanography*, *26*(2), 191–195.
Mitchell, M., C. Hershner, J. Herman, D. Schatt, E. Eggington, and S. Stiles (2013), *Recurrent flooding study for Tidewater Virginia, Rep. SJR 76, 2012*, 141 pp., Va. Inst. of Marine Sci., Gloucester Point, Va.
Nicholls, R. J., and A. Cazenave (2010), Sea-level rise and its impact on coastal zones, *Science*, *328*(5985), 1517–1520.
Rossby, T., C. N. Flagg, K. Donohue, A. Sanchez-Franks, and J. Lillibridge (2014), On the long-term stability of Gulf Stream transport based on 20 years of direct measurements, *Geophys. Res. Lett.*, *41*, 114–120, doi:10.1002/2013GL058636.
Sallenger, A. H., K. S. Doran, and P. Howd (2012), Hotspot of accelerated sea-level rise on the Atlantic coast of North America, *Nat. Clim. Change*, *2*, 884–888, doi:10.1038/ncilmate1597.
Smeed, D. A., et al. (2013), Observed decline of the Atlantic Meridional Overturning Circulation 2004 to 2012, *Ocean Sci. Discuss.*, *10*, 1619–1645.
Srokosz, M., M. Baringer, H. Bryden, S. Cunningham, T. Delworth, S. Lozier, J. Marotzke, and R. Sutton (2012), Past, present, and future changes in the Atlantic meridional overturning circulation, *Bull. Am. Meteorol. Soc.*, *93*, 1663–1676, doi:10.1175/bams-d-11-00151.1.
Sweet, W., C. Zervas, and S. Gill (2009), Elevated east coast sea level anomaly: June-July 2009, *NOAA Tech. Rep. No. NOS CO-OPS 051*, 40 pp., NOAA Natl. Ocean Service, Silver Spring, Md.
Yin, J., and P. B. Goddard (2013), Oceanic control of sea level rise patterns along the East Coast of the United States, *Geophys. Res. Lett.*, *40*, 5514–5520, doi:10.1002/2013GL057992.

Yin, J., M. E. Schlesinger, and R. J. Stouffer (2009), Model projections of rapid sea-level rise on the northeast coast of the United States, *Nat. Geosci.*, *2*, 262–266, doi:10.1038/ngeo462.

Zervas, C. (2009), Sea level variations of the United States 1854-2006. *NOAA Tech. Rep. NOS CO-OPS 053*, 78 pp., NOAA/Natl. Ocean Service, Silver Spring, Md.

Zhang, H., and J. Sheng (2013), Estimation of extreme sea levels over the eastern continental shelf of North America, *J. Geophys. Res. Oceans*, *118*, 6253–6273, doi:10.1002/2013JC009160.

Zhang, K. (2011), Analysis of non-linear inundation from sea-level rise using LIDAR data: A case study for south Florida, *Clim. Change*, *106*, 535–565, doi:10.1007/s10584-010-9987-2.

Zhao, J., and W. Johns (2014), Wind-forced interannual variability of the Atlantic Meridional Overturning Circulation at 26.5°N, *J. Geophys. Res. Oceans*, *119*, 6253–6273, doi:10.1002/2013JC009407.